HHS Public Access

Author manuscript

Mater Sci Eng C Mater Biol Appl. Author manuscript; available in PMC 2017 October 01.

Published in final edited form as:

Mater Sci Eng C Mater Biol Appl. 2016 October 01; 67: 59–64. doi:10.1016/j.msec.2016.04.093.

Single Step Synthesis, Characterization and Applications of Curcumin Functionalized Iron Oxide Magnetic Nanoparticles

Rohit Bhandari, **Prachi Gupta**, **Thomas Dziubla**, and **J. Zach Hilt***

Chemical and Materials Engineering Department, University of Kentucky, Lexington, KY 40506

Abstract

Magnetic iron oxide nanoparticles have been well known for their applications in magnetic resonance imaging (MRI), hyperthermia, targeted drug delivery, etc. The surface modification of these magnetic nanoparticles has been explored extensively to achieve functionalized materials with potential application in biomedical, environmental and catalysis field. Herein, we report a novel and versatile single step methodology for developing curcumin functionalized magnetic Fe_3O_4 nanoparticles without any additional linkers, using a simple coprecipitation technique. The magnetic nanoparticles (MNPs) were characterized using transmission electron microscopy, x-ray diffraction, fourier transform infrared spectroscopy and thermogravimetric analysis. The developed MNPs were employed in a cellular application for protection against an inflammatory agent, a polychlorinated biphenyl (PCB) molecule.

Graphical Abstract

Novel single step curcumin coated magnetic Fe_3O_4 nanoparticles without any additional linkers for cell viability applications

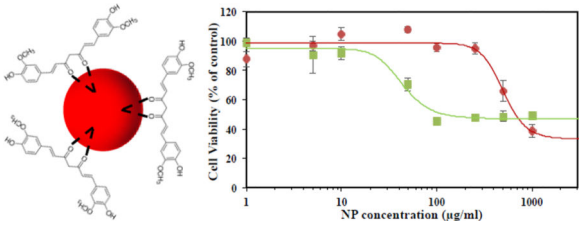

Keywords

Curcumin; Iron oxide; Functionalization; Cell viability; Anti-inflammatory

1. INTRODUCTION

Magnetic iron oxide (Fe_3O_4) nanoparticles have attracted tremendous attention in the last few decades due to their ease of preparation, minimal toxicity with appropriate surface functionalization, and the ability of rapid magnetic separation.[1,2] In addition, Fe_3O_4 magnetic nanoparticles (MNPs) have shown promising application as materials of interest

* zach.hilt@uky.edu, Phone: 859-257-9844, Fax: 859-323-1929.

for ferrofluids,[3,4] hyperthermia,[5] magnetic resonance imaging (MRI),[6,7] high-density information storage,[8] and targeted drug delivery labeling.[9] A variety of methodologies including coprecipitation, sol-gel method, thermal decomposition, microemulsion and hydrothermal synthesis have been reported for the synthesis of Fe_3O_4 MNPs, and further advancement in the synthesis of such materials is still on-going due to their outstanding potential in variety of applications.[10–14] Among these, coprecipitation technique is a well-known method for the synthesis of Fe_3O_4 MNPs using Fe^{2+}/Fe^{3+} as precursors under high-temperature conditions (85–90 °C) in the presence of a base.[1,15,16] The method generally results in the formation of smaller core particles of size around 10–12 nm; however, the size could be further modulated using alternative synthetic approaches such as thermal decomposition.[17] The unique feature of these Fe_3O_4 MNPs lies in the ease of magnetic separation such that these particles could be functionalized as a catalyst for a specific chemical reaction, followed by an easy magnetic decantation process to ensure recyclability. A variety of stabilizing agents have also been reported in the literature being used for the coprecipitation of Fe_3O_4 nanoparticles, allowing the introduction of additional functionality on the nanoparticle surface.[18–20] Such methodologies could modify the magnetic nanoparticle surface with exposed functional groups that could lead to the desired uniform dispersion of the particles in an aqueous environment and hence could be easily tailored for many potential applications. In reference to these systems, citrate-coated, dextran-modified, and self-assembled monolayer-coated Fe_3O_4 MNPs have been prepared and find extensive application in biomedical, environmental, and catalysis field.[18,19,21–23]

For these active areas of research, magnetic nanomaterials could have major applications, especially in the field of medicine and environmental remediation. The present study describes the synthesis of surface modified MNPs that could potentially be utilized for such applications. Fe_3O_4 MNPs with surface functional groups could be attached to bioactive molecules and thus could be targeted to the required site depending upon the application.[9,18,24] Extensive research is still on going to develop such functionalized nanomaterials under ambient conditions. In context of various functional groups interacting with the nanoparticle surface, curcumin, a naturally occurring dietary component and polyphenolic molecule, has been widely documented in the literature.[25–27] Curcumin is known to have antiseptic and anti-inflammatory properties, along with several other therapeutic properties.[28,29,30] Although curcumin has low bioavailability, it has been reported that conjugation of curcumin with metal nanoparticles could increase its bioavailability.[31] Also, based on previously reported spectroscopic measurements at various temperatures, the breaking of intra-molecular H-bonding could increase the solubility of curcumin in water at higher temperatures.[32] The molecular structure of curcumin possesses multiple aromatic groups with hydroxyl functionalities that could be utilized for interaction with other aromatic molecules such as polychlorinated biphenyls (PCBs) via pi-pi stacking interactions. Such interaction could be further employed to capture and sense toxic pollutants such as PCBs from environmental samples. Rajaram et al. have recently demonstrated the synthesis of zerovalent curcumin conjugated gold nanoparticles under room temperature conditions using curcumin as both reducing and stabilizing agent.[33] In a similar study, Kundu and co-workers have shown the synthesis of curcumin stabilized Ag nanoparticles and their application in surface enhance Raman spectroscopy (SERS) using

methylene blue as Raman probe.[31] Kale and coworkers have also designed a Fe_3O_4-citric acid-curcumin conjugated nanoplatform with application in superoxide scavenging, tumor suppression and cancer hyperthermia.[25] Many reports of curcumin conjugation with Fe_3O_4 nanoparticles have been reported in literature with an additional linker to modify the nanoparticle surface with curcumin; however, a direct functionalization in single step without any linkers and additional reaction steps has not been reported to date.[25,34]

In the present study, we describe a novel and versatile single step methodology for the synthesis of curcumin stabilized Fe_3O_4 magnetic nanoparticles (C-IO MNPs) in aqueous solution by a simple co-precipitation method (Figure 1). The materials were characterized using transmission electron microscopy (TEM), thermogravimetric analysis (TGA), X-ray diffraction (XRD), Fourier transform infrared spectroscopy (FTIR) and dynamic light scattering (DLS). The synthesized curcumin-Fe_3O_4 nanoparticles were then analyzed for cell viability assay against PCB126 toxicity.

2. EXPERIMENTAL

Materials

Iron (III) chloride hexahydrate ($FeCl_3.6H_2O$), iron (II) chloride ($FeCl_2.4H_2O$) and dimethyl sulfoxide (DMSO) were obtained from Sigma-Aldrich, while the ammonium hydroxide (NH_4OH) was procured from EMD Chemicals. Curcumin powder was purchased from Chem-Impex Int'l Inc. For cell culture studies, EBM basal medium (phenol red free), EGM-2 growth factors, and Human Umbilical Vein Endothelial Cells were purchased from Lonza. Calcein-AM red-orange was purchased from Life Technologies. All chemicals were used as received.

Synthesis of C-IO MNPS

Curcumin coated iron oxide nanoparticles were prepared using a novel and simple coprecipitation method. An aqueous solution of Fe (III) and Fe(II) salts was prepared in a molar ratio of 2:1 and the reaction was setup under an inert atmosphere (nitrogen). In a specific reaction, 2.2 g of $FeCl_3.6H_2O$ and 0.8 g of $FeCl_2.4H_2O$ were dissolved in 40.0 mL of water in a three neck round bottom flask and the reaction was setup under a constant nitrogen flow. The reaction was heated and 10.0 weight % of curcumin (dissolved in DMSO) was added dropwise to the reaction system around 40 °C. The reaction was then set to a specific temperature (85 °C) and 5.0 mL of 28% (w/w) ammonium hydroxide was added to the reaction with vigorous stirring at a set temperature. The reaction was then allowed to stir at 85 °C for about one hour, followed by magnetic decantation and washing steps using ethanol, 50:50 acetonitrile/dichloromethane and water.

Characterization

XRD analysis was carried out using a Bruker-AXS D8 DISCOVER diffractometer with a CuKa radiation source.

Attenuated total reflectance FTIR (ATR-FTIR) was used to investigate the presence of characteristic curcumin functional groups coated on the nanoparticle surface using a Varian

7000e FTIR spectrophotometer. Dried powders of samples were placed on a diamond ATR crystal and the IR spectrum was recorded. The spectrum was obtained between 800 and 3600 cm^{-1} using 32 scans.

TEM images of samples were obtained using a JEOL 2010 FX with an accelerating voltage of 200kV. The samples for analysis were prepared by drying a drop (~5.0 μL) of the particles dispersed in DI water onto a lacey carbon grid.

DLS measurements were conducted using a Malvern Nanoseries Zetasizer (Nano-ZS90). The samples were prepared in water and 10.0 mM NaCl solution at a concentration of 200 μg/mL.

A Q500 TA instrument was used for the TGA measurements. All the measurements were conducted under a constant flow of nitrogen. 10 to 20 mg of sample was used at a heating rate of 5 °C/min. The sample was isothermally heated for 20 min at 120 °C to completely remove any residual water components. The sample was further heated till 600 °C to degrade the polyphenolic coating. The final TGA curves obtained were normalized with respect to the weight at 120 °C.

Dose dependent in vitro toxicity of nanoparticles

Human umbilical vein endothelial cells (HUVECs) were seeded to 80% confluency in a Falcon 96-well plate for overnight. Cells were treated with 200 μL uncoated IO NPs **(Frimpong et al. 2010)** or C-IO NPs suspension in the EBM-2 basal medium at concentrations ranging from 1 to 1000 μg/mL. After 24.0 h of NPs treatment, NP suspension media in each well was removed, wells were washed with fresh media once, followed by the incubation of cells in 1.0 μM calcein AM red-orange live cell tracer dye. Calcein AM red-orange is a fluorescent cell permeable live cell tracer dye, acetomethoxy bond of which is cleaved via ester hydrolysis in the presence of intracellular esterases of live cells. An hour later, media was removed again, washed once with fresh media followed by addition of 200 μL of media again. The well-plate was then read for fluorescence intensity with 540/590 nm as excitation/emission wavelength using BioTek Synergy Mx, Gen5 2.0, Winooski, VT. Percent cell viability was calculated by taking fluorescence intensity of non-treated control group as 100% viability. Fluorescent images of the treated HUVECs after calcein AM red-orange dye incubation were taken using a Nikon Eclipse LV100D-U microscope with Texas Red excitation filter.

PCB 126 exposure studies

To assess the protective effect of C-IO NPs on PCB induced toxicity, HUVECs at 80% confluency were pre-treated with 10 μg/mL C-IO NPs suspended in cell culture media for 0, 12 and 24-hour followed by addition of 10 μL of 1.0 mM PCB 126. PCB 126 stock solution was prepared by adding 100 μL of 10 mM PCB 126 solution in DMSO to 900 μL of EBM-2 basal medium and mixing. After 24.0 h exposure of PCB 126 post C-IO NP pre-treatment, cells were washed with fresh media followed by incubation in 1.0 μM calcein AM red-orange solution prepared in the EBM-2 basal medium. One hour later, cells were washed

again and 200 μL of fresh media was added to each well. The plate was again read at 540/590 nm excitation/emission wavelengths to calculate percent viability.

3. RESULTS AND DISCUSSION

The synthesis method for developing curcumin stabilized Fe_3O_4 nanoparticles has been presented in Figure 1. A mixture of Fe (III) and Fe (II) salts was dissolved in aqueous medium and the reaction was setup in a sealed environment under nitrogen with a heating probe. The reaction mixture was allowed to stir with increasing temperature and a 10.0 weight % curcumin solution in DMSO was added to the reaction at the attained temperature of 40 °C. Further, when the reaction system reached the set temperature of 85 °C, 5.0 mL of NH_4OH solution (28% v/v) was added that resulted in immediate black precipitate suggesting the formation of Fe_3O_4 MNPs. The reaction was allowed to continue at 85 °C for additional 1.0 h and was followed by triplicate washes with ethanol, water, as well as 50:50 acetonitrile/dichloromethane using magnetic decantation to achieve curcumin stabilized Fe_3O_4 nanoparticles. The obtained nanoparticles were then fully characterized using a variety of analytical techniques.

Figure 2a shows the XRD spectrum for the curcumin stabilized Fe_3O_4 nanoparticles. The diffraction peak originates from (111), (220), (311), (400), (422), (511) and (440) planes over a 2θ range (5–65 degrees), confirming the magnetite (Fe_3O_4) structure for the nanoparticle system, as matched with JDPCS card (19-0629). Scherer analysis was used to calculate the crystallite size using the (311) peak, resulting in average particle size of approximately 8.1 nm. The intensity of the (311) peak was observed to be higher in comparison to other peaks. Here, curcumin is directly employed as a stabilizing agent on the surface of Fe_3O_4 MNPs.

Hence, the interaction of curcumin with the different facets of nanoparticle surface could reduce or enhance the growth rate of certain planes along specific directions, resulting in such variation in peak intensity from the XRD analysis. Thermal properties and composition for both uncoated and curcumin stabilized Fe_3O_4 nanoparticles as well as pure curcumin were measured using thermogravimetric analysis (TGA) as presented in Figure 2b. Uncoated Fe_3O_4 nanoparticles do not show any significant weight loss in the temperature range of measurement (120 – 500 °C).

A prominent weight loss of ~12.4% was noted for curcumin Fe_3O_4 nanoparticles between 120 – 600 °C temperature range that could be attributed to the curcumin loss during the measurement. Also, the curcumin degradation on the nanoparticle surface occurs at a higher temperature, possibly due to its interaction with the surface that could delay the organic degradation.[35] Previously, it has been shown that raw curcumin undergoes gradual thermal decomposition in a stage-wise manner where stage (I) occurs between the temperature range of 94–357 °C due to the degradation of substituent groups of curcumin and stage (II) follows from temperature range of 357–533 °C owing to the decomposition of two benzene rings in curcumin.[36] From figure 2b, we also observe similar degradation pattern for pure curcumin resulting in extensive mass loss over a high-temperature range. In another study, Mathew et al also demonstrated that pure curcumin start degrading around 200 °C, while curcumin

conjugated with poly (lactic-co-glycolic acid) (PLGA) nanoparticles occurs rapidly at higher temperature (~300 °C).[37] Thus, the interaction of curcumin with the nanoparticle surface via the keto-enol functionality would likely increase its thermal stability and could delay the degradation of organic coating to higher temperature range, as observed in our study.

The hydrodynamic size of the C-IO nanoparticles was determined using DLS and is presented in Table 1. The C-IO nanoparticles had an average size of 406 ± 13 nm with a PDI of 0.244 in DI water and a slightly increased average size of 458 ± 39 nm with a PDI of 0.137 in 10.0 mM NaCl at room temperature conditions. The average size determination was based on triplicate sample analysis in both solvent systems. TEM analysis was further conducted for the C-IO MNPs. Previously, other groups and our group have reported the synthesis of uncoated Fe_3O_4 nanoparticles via coprecipitation method, where an average size of approximately 10–12 nm was reported for the core uncoated Fe_3O_4 particles.[15,38] For the C-IO MNPs, TEM analysis is presented in Figure 3a and 3b, where an average size of 9.9 ± 1.3 nm was observed for the synthesized particles using an average analysis of a random selection of approximately 100 nanoparticles. The average nanoparticle size for the curcumin stabilized MNPs does not show a significant difference in size as compared to the uncoated nanoparticles, further suggesting that synthetic process did not alter the particle morphology. Also, TEM images for C-IO MNPs shown in Figure 3a and 3b show the presence of individual particles that tends to agglomerate, resulting in larger aggregates. Figure 3c presents the Fourier transform infrared (FTIR) spectra for uncoated, pure curcumin and curcumin stabilized Fe_3O_4 nanoparticles. The functionalization/specific interaction of curcumin with the Fe_3O_4 nanoparticle surface was investigated using the FTIR spectrum of pure curcumin with the functionalized Fe_3O_4 nanoparticles. The uncoated and C-IO MNPs were dried, and solid samples were directly used for the FTIR analysis. A detailed FTIR analysis suggests the binding/interaction of curcumin to the nanoparticle surface and nature of the interaction between them. The spectrum for the uncoated Fe_3O_4 nanoparticles (black trace in Figure 3c) does not reveal any significant features and is consistent with the previously reported literature. The spectrum for curcumin stabilized Fe_3O_4 MNPs (blue trace) shows the presence of new peaks in comparison to the uncoated nanoparticles, suggesting an interaction with curcumin. To further corroborate the interaction, the peak at 963 cm^{-1} in pure curcumin spectrum corresponds to the in-plane bending of the hydroxyl group of the enolic moiety,[33] which disappears in the blue spectrum (C-IO MNPs) suggesting functionalization via the keto-enol functionality in the curcumin backbone. Prior studies have also shown similar interaction, where metal nanoparticles such as Au and Ag were functionalized with curcumin via the keto-enol functionality in aqueous solution.[31,33] A broad peak around 3290 cm^{-1} and a sharp peak around 3470 cm^{-1} in pure curcumin spectrum indicate the presence of –OH functional groups,[39] which could also be seen in curcumin functionalized Fe_3O_4 nanoparticle spectrum around 3500–3200 cm^{-1}. The presence of strong peak around 1605 cm^{-1} in pure curcumin spectrum corresponds to predominantly mixed ν(C=C) and ν(C=O) character.[39] However, this peak seems to be subdued in intensity and shifted to around 1573 cm^{-1} suggesting an interaction of curcumin with the nanoparticle surface. Also, the peak at 1023 cm^{-1} in pure curcumin is assigned to the C-O-C stretching that could also be seen in the blue trace (with lower intensity) further suggesting the presence of intact C_6H_5-O-CH_3 moieties in the curcumin functionalized

nanoparticle system, indicating curcumin functionalization on the particle surface.[39] Hence, we can confirm the MNP surface has been functionalized by curcumin, where curcumin also acts as a stabilizing agent for the Fe_3O_4 MNPs.

In addition to the physicochemical characterization of C-IO MNPs, the nanoparticles were tested in cell viability studies where they successfully demonstrated protection against an inflammatory agent in a cellular system as tested with human umbilical vein endothelial cells (HUVECs), (Figure 4). HUVECs when incubated with curcumin coated iron oxide MNPs (C-IO MNPs) for 24.0 h and effectively showed less cell death relative to uncoated iron oxide MNPs[14] at variable concentrations. This was verified by carrying out a calcein AM red-orange viability assay, which is a live cell quantifying fluorescence probe (excitation/emission at 540/590 nm). The C-IO MNPs nanoparticles had a TC_{50} value of 500 μg/mL, while the uncoated iron oxide MNPs demonstrated 50% cell death at only 50 μg/mL (Figure 4a). The increased protection against IO toxicity is potentially due to the antioxidant response of curcumin against the inflammatory effects of iron oxide nanoparticles as has been shown earlier in the literature with poly(trolox) nanoparticles.[40] Also, with 10–12 wt/wt% curcumin loading, TC_{50} based upon equivalent curcumin loading comes out to be about 50–60 μg/mL. This represents a 10-fold higher value than for pure curcumin (TC_{50}~5 μg/mL), thereby increasing the limits for safe administrative concentrations. The inset in Figure 4a shows the fluorescent images of the HUVECs for two concentrations of C-IO MNPs after 24-hour exposure followed by calcein AM red-orange dying. In addition, the C-IO MNPs also demonstrated a protective effect against polychlorinated biphenyl 126 (PCB126) exposure, which is an inflammatory agent (Figure 4b), mostly due to the antioxidant content in the nanoparticles. With 12.0 or 24.0 h prior incubation of 10.0 μg/mL of C-IO MNPs nanoparticles with HUVECs followed by exposure of cells to PCB126 at a concentration 50.0 μM, there was a significant difference between curcumin stabilized Fe_3O_4 MNPs treated and non-treated cells. While PCB126 control showed a cell viability of 49 ± 2.3 %, cells treated with C-IO MNPs at 12.0 and 24.0 hours prior to PCB126 exposure showed 54 ± 2.4 % and 70 ± 6.8 % viability, respectively. Curcumin has been extensively investigated for its antioxidant properties, and continuous efforts are being made in order to deliver it in active functional form. This unique nanoparticle system can help achieve this aim. With the efforts being made in improving the biocompatibility in the field of iron oxide MNPs, the synthesized antioxidant coated/surface functionalized C-IO MNPs demonstrated a significant improvement in cell viability.

A possible explanation for this could be the antioxidant activity of the curcumin on the surface of the MNP and the coating providing a barrier to direct interaction of the iron oxide MNP surface with the cell and cellular components. In addition, anti-inflammatory protection against PCB126 exposure upon prior incubation of C-IO MNPs with HUVECs was observed. PCBs are persistent and potent environmental pollutants, and many efforts are being made to eradicate these from the environment as well protect from their toxic effects (e.g., carcinogenic effects) when absorbed into the body.[41,42] Based on multiple inflammatory studies on PCBs being conducted by numerous research groups, it is thought that they diffuse into cells within 1.0 hour of exposure. A proposed mechanism of protection due to the C-IO MNPs, which is greatest upon prior incubation, is that the nanoparticles need time to transport into the cells to be most effective in protecting against the insult. The

ability of C-IO MNPs to protect against PCBs could be due to the PCBs binding and adsorption to the surface due to pi-pi interaction and/or cell protection against the oxidative effects due to the activity of the curcumin on the surface of the MNPs. Further studies are underway to further characterize the mechanism of protection.

4. CONCLUSIONS

To summarize, we have described a novel and versatile single step methodology for the synthesis of curcumin stabilized Fe_3O_4 nanoparticles using a coprecipitation technique. The materials were fully characterized showing the functionalization of curcumin with Fe_3O_4 nanoparticle surface. The application of these materials in the protection against an inflammatory agent was also demonstrated. The current approach of functionalizing Fe_3O_4 nanoparticles with curcumin has many potential applications in medicine, environmental remediation, and other fields.

Acknowledgments

The project described was supported by Grant Number P42ES007380 from the National Institute of Environmental Health Sciences (NIEHS). The content is solely the responsibility of the authors and does not necessarily represent the official views of the National Institute of Environmental Health Sciences or the National Institutes of Health.

REFERENCES

1. Mascolo M, Pei Y, Ring T. Materials. 2013; 6:5549–5567.
2. Yen SK, Varma DP, Guo WM, Ho VHB, Vijayaragavan V, Padmanabhan P, Bhakoo K, Selvan ST. Chem. – Eur. J. 2015; 21:3914–3918. [PubMed: 25630810]
3. Brullot W, Reddy NK, Wouters J, Valev VK, Goderis B, Vermant J, Verbiest T. J. Magn. Magn. Mater. 2012; 324:1919–1925.
4. Mandel K, Straßer M, Granath T, Dembski S, Sextl G. Chem. Commun. 2015; 51:2863–2866.
5. Moroz P, Jones SK, Gray BN. Int. J. Hyperthermia. 2002; 18:267–284. [PubMed: 12079583]
6. Sun C, Lee JSH, Zhang M. Inorg. Nanoparticles Drug Deliv. 2008; 60:1252–1265.
7. Moradi S, Akhavan O, Tayyebi A, Rahighi R, Mohammadzadeh M, Saligheh Rad HR. RSC Adv. 2015; 5:47529–47537.
8. Reiss G, Hutten A. Nat. Mater. 2005; 4:725–726. [PubMed: 16195762]
9. Lubbe AS, Alexiou Christoph, Bergemann Christian. J. Surg. Res. 2001; 95:200–206. [PubMed: 11162046]
10. Si S, Li C, Wang X, Yu D, Peng Q, Li Y. Cryst. Growth Des. 2005; 5:391–393.
11. Sun S, Zeng H. J. Am. Chem. Soc. 2002; 124:8204–8205. [PubMed: 12105897]
12. Tang NJ, Zhong W, Jiang HY, Wu XL, Liu W, Du YW. Int. Symp. Adv. Magn. Technol. 2004; 282:92–95.
13. Li G, Jiang Y, Huang K, Ding P, Chen J. J. Alloys Compd. 2008; 466:451–456.
14. Daou TJ, Pourroy G, Bégin-Colin S, Grenèche JM, Ulhaq-Bouillet C, Legaré P, Bernhardt P, Leuvrey C, Rogez G. Chem. Mater. 2006; 18:4399–4404.
15. Frimpong RA, Dou J, Pechan M, Hilt JZ. J. Magn. Magn. Mater. 2010; 322:326–331.
16. Wydra RJ, Oliver CE, Anderson KW, Dziubla TD, Hilt JZ. RSC Adv. 2015; 5:18888–18893. [PubMed: 25798231]
17. Park J, An K, Hwang Y, Park J-G, Noh H-J, Kim J-Y, Park J-H, Hwang N-M, Hyeon T. Nat. Mater. 2004; 3:891–895. [PubMed: 15568032]
18. Răcuciu M, Creangă DE, Airinei A. Eur. Phys. J. E. 2006; 21:117–121. [PubMed: 17180642]

19. Hong RY, Feng B, Chen LL, Liu GH, Li HZ, Zheng Y, Wei DG. Biochem. Eng. J. 2008; 42:290–300.
20. Wang S, Zhang Z, Liu B, Li J. Catal. Sci. Technol. 2013; 3:2104–2112.
21. Correa-Duarte MA, Giersig M, Kotov NA, Liz-Marzán LM. Langmuir. 1998; 14:6430–6435.
22. Frimpong, Reynolds A., Hilt, J Zach. Nanotechnology. 2008; 19:175101. [PubMed: 21825659]
23. Kruse AM, Meenach SA, Anderson KW, Hilt JZ. Acta Biomater. 2014; 10:2622–2629. [PubMed: 24486913]
24. Mahdavi M, Ahmad M, Haron M, Namvar F, Nadi B, Rahman M, Amin J. Molecules. 2013; 18:7533–7548. [PubMed: 23807578]
25. Kitture R, Ghosh S, Kulkarni P, Liu XL, Maity D, Patil SI, Jun D, Dushing Y, Laware SL, Chopade BA, Kale SN. J. Appl. Phys. 2012; 111:064702.
26. Borsari M, Ferrari E, Grandi R, Saladini M. Inorganica Chim. Acta. 2002; 328:61–68.
27. Mulik R, Mahadik K, Paradkar A. Eur. J. Pharm. Sci. 2009; 37:395–404. [PubMed: 19491031]
28. Wilken R, Veena M, Wang M, Srivatsan E. Mol. Cancer. 2011; 10:12. [PubMed: 21299897]
29. Nagpal M, Sood S. J. Nat. Sci. Biol. Med. 2013; 4:3–7. [PubMed: 23633828]
30. Hatamie S, Akhavan O, Sadrnezhaad SK, Ahadian MM, Shirolkar MM, Wang HQ. Mater. Sci. Eng. C. 2015; 55:482–489.
31. Kundu S, Nithiyanantham U. RSC Adv. 2013; 3:25278–25290.
32. Singh DK, Jagannathan R, Khandelwal P, Abraham PM, Poddar P. Nanoscale. 2013; 5:1882–1893. [PubMed: 23348618]
33. Sindhu K, Rajaram A, Sreeram KJ, Rajaram R. RSC Adv. 2014; 4:1808–1818.
34. Wani KD, Kitture R, Ahmed A, Choudhari AS, Koppikar SJ, Kale SN, Kaul-Ghanekar R. J. Bionanoscience. 2011; 5:59–65.
35. Unal B, Durmus Z, Kavas H, Baykal A, Toprak MS. Mater. Chem. Phys. 2010; 123:184–190.
36. Chen Z, Xia Y, Liao S, Huang Y, Li Y, He Y, Tong Z, Li B. Food Chem. 2014; 155:81–86. [PubMed: 24594157]
37. Mathew A, Fukuda T, Nagaoka Y, Hasumura T, Morimoto H, Yoshida Y, Maekawa T, Venugopal K, Kumar DS. PLoS ONE. 2012; 7:e32616. [PubMed: 22403681]
38. Mohammadi-Samani S, Miri R, Salmanpour M, Khalighian N, Sotoudeh S, Erfani N. Res. Pharm. Sci. 2013; 8:25–33. [PubMed: 24459473]
39. Mohan PRK, Sreelakshmi G, Muraleedharan CV, Joseph R. Vib. Spectrosc. 2012; 62:77–84.
40. Cochran DB, Wattamwar PP, Wydra R, Hilt JZ, Anderson KW, Eitel RE, Dziubla TD. Biomaterials. 2013; 34:9615–9622. [PubMed: 24016851]
41. van den Dungen MW, Rijk JCW, Kampman E, Steegenga WT, Murk AJ. Toxicol. In Vitro. 2015; 29:769–778. [PubMed: 25765474]
42. Rignall B, Grote K, Gavrilov A, Weimer M, Kopp-Schneider A, Krause E, Appel KE, Buchmann A, Robertson LW, Lehmler H-J, Kania-Korwel I, Chahoud I, Schwarz M. Toxicol. Sci. 2013; 133:29–41. [PubMed: 23457121]

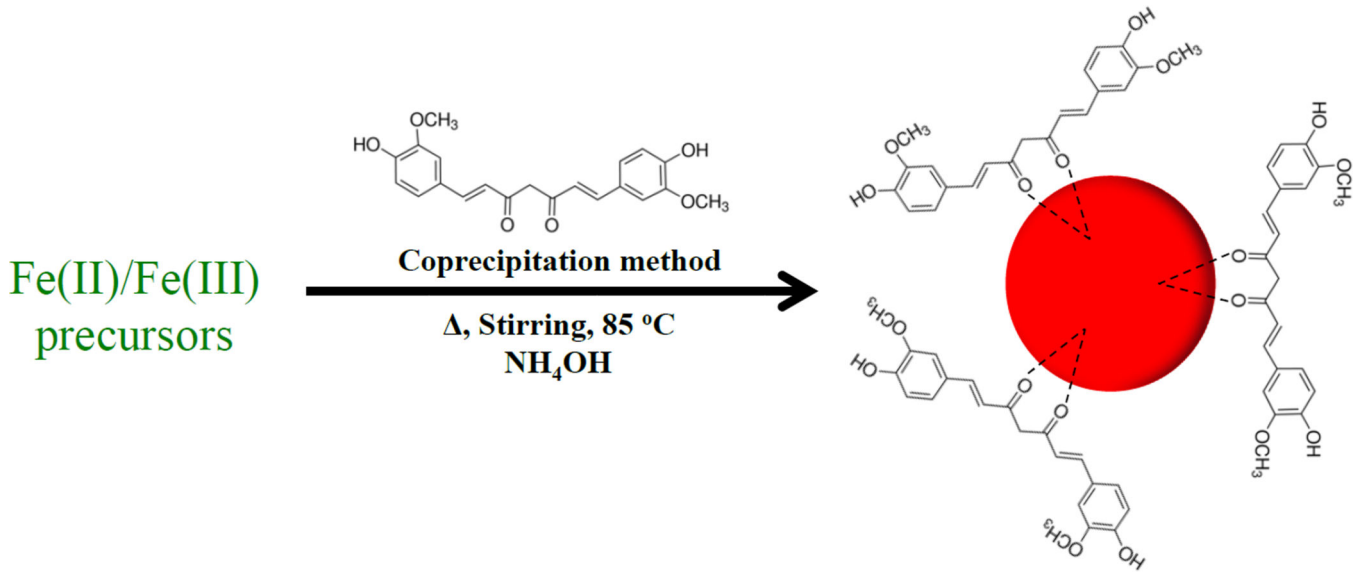

Fig. 1.

Represents the synthesis method for Curcumin functionalized magnetic Fe_3O_4 nanoparticles.

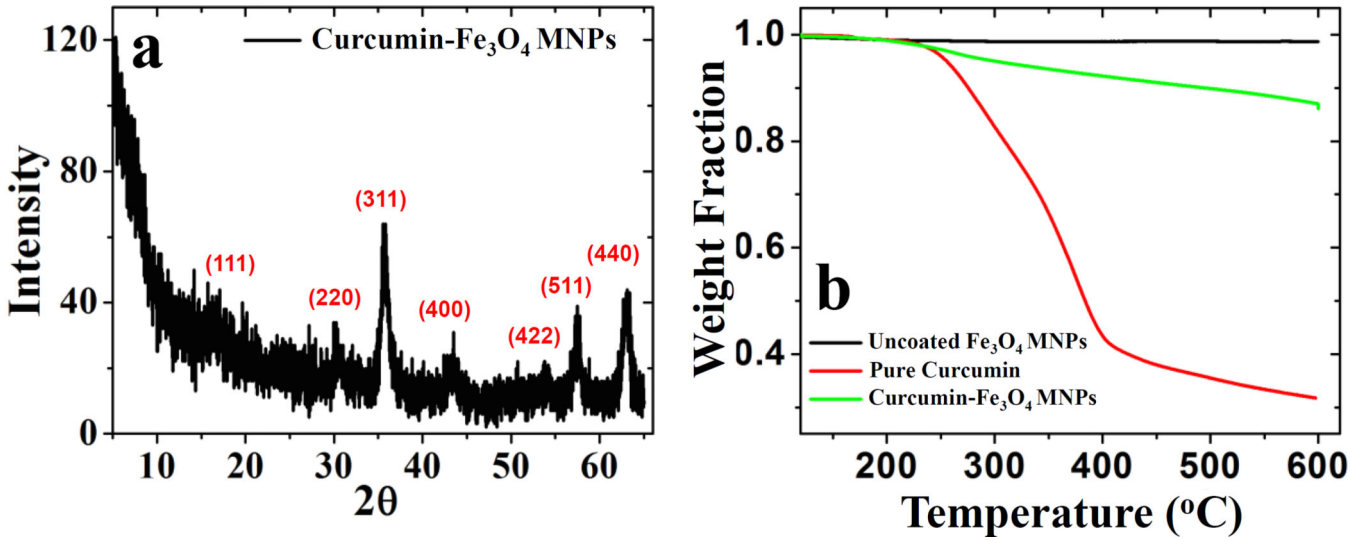

Fig. 2.

Part (a) shows the XRD spectrum for C-IO MNPs and (b) presents the TGA profile for uncoated and C-IO MNPs.

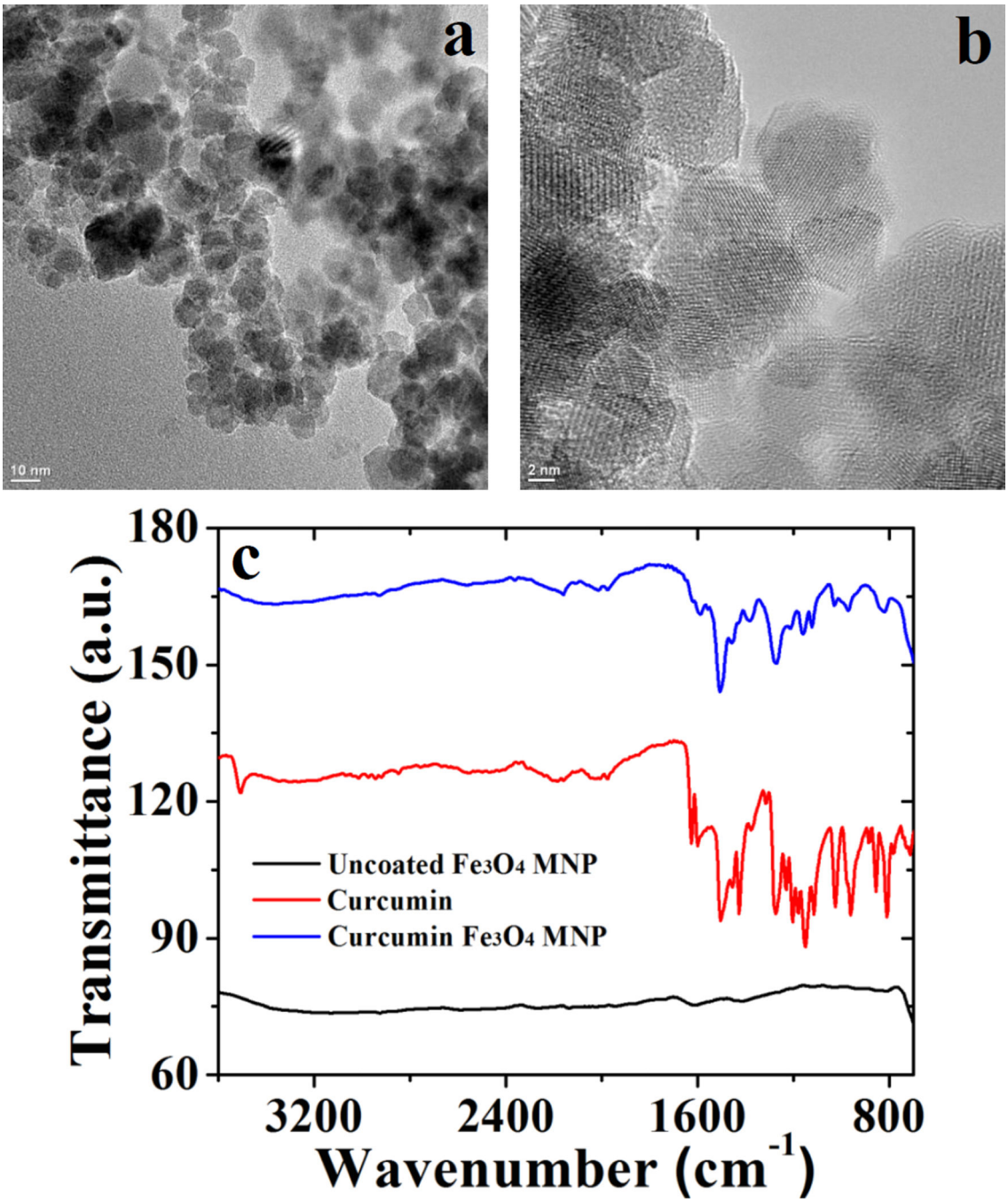

Fig. 3.

Presents the TEM micrographs for C-IO MNPs (part a and b), while c) shows the individual FTIR spectrum for uncoated IO, pure curcumin and C-IO MNPs, respectively.

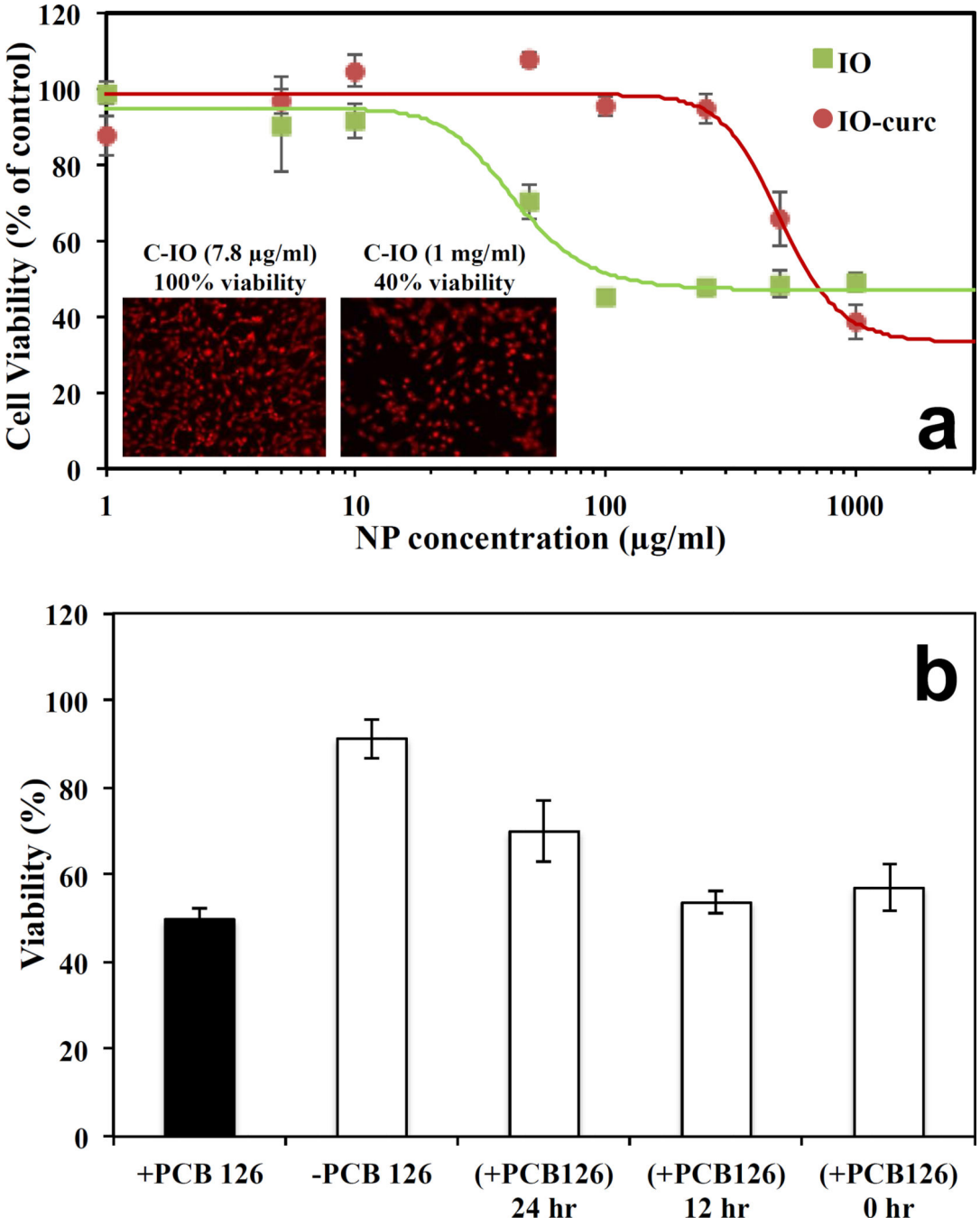

Fig. 4.

Shows the cell viability assay analysis using C-IO MNPs. Part a) Dose dependent exposure of uncoated iron oxide and curcumin-iron oxide nanoparticles towards HUVECs for 24 hours followed by viability analysis using Calcein AM red-orange live cell tracer. *Inset: Fluorescent images of the HUVECs after 24-hour exposure followed by calcein AM red-orange dying*. Part b) Protection against PCB 126 induced inflammation. HUVECs

preincubated with 10 μg/mL curcumin iron oxide nanoparticles for 0, 12 and 24 hours followed by 24-hour exposure to 50 μM PCB126.

Table 1

Showing the particle size analysis for C-IO magnetic nanoparticles in water and 10.0 mM NaCl system.

System	Particle size (nm) in water[a]	PDI	Particle size (nm) in 10.0 mM NaCl[a]	PDI
C-IO MNPs	406 ± 13	0.244	458 ± 39	0.137

[a]The particle size was calculated using three different sample batches